

# First measurement from Charmless $B$ Decays at Belle II

---

Yun-Tsung Lai<sup>\*†</sup>

Kavli IPMU

E-mail: [yun-tsung.lai@ipmu.jp](mailto:yun-tsung.lai@ipmu.jp)

We report on first measurement of branching fractions ( $\mathcal{B}$ ) and  $CP$  asymmetries ( $\mathcal{A}$ ) in various charmless  $B$  decays at Belle II. We utilize a data sample of  $34.6 \text{ fb}^{-1}$  which is collected in SuperKEKB  $e^+e^-$  collider at the  $\Upsilon(4S)$  resonance in 2019 and 2020. The analysis procedures, including the Monte Carlo (MC) simulation study, background reduction, and physics observable measurements, will be described in detail in this report. Polarization fraction of  $B \rightarrow \phi K^*$  modes is also measured. All these results in charmless  $B$  decays from Belle II are consistent with world average and are good validations on the detector systems and analysis strategies. Belle II is ready for more new physics search with larger data set in near future in all aspects.

*The 19th International Conference on B-Physics at Frontier Machines (BEAUTY 2020)*

*21-24 September, 2020*

*Remote conference*

---

<sup>\*</sup>Speaker.

<sup>†</sup>On behalf of the Belle II Collaboration.

## 1. Introduction

The charmless  $B$  decay is an important field for new physics (NP) in flavor sector. The decays via penguin diagram are sensitive to non-Standard-Model components contributing to the penguin loop. The determination on  $\phi_2/\alpha$  by the combined measurement on branching fractions and  $CP$  asymmetries of all  $B \rightarrow \pi\pi$  isospin modes [1] is one of the experimental approach, while any discrepancy from the SM prediction can be an indication to NP. The isospin sum rule also provides constraints on the branching fractions and  $CP$  asymmetries of the  $B \rightarrow K\pi$  modes, which is called  $B \rightarrow K\pi$  puzzles [2]. Any violation on the sum rule is also a clear hint to new physics. The three-body charmless  $B$  decays, due to the interference between different decay amplitudes, are sensitive to  $CP$  asymmetry localized in the phase space. By a full Dalitz plot analysis, we can search for localized  $CP$  asymmetry, the intermediate resonance, constrain magnitudes and phases of the CKM matrix elements.

For the penguin-dominant  $B^0 \rightarrow \phi K^0$  mode, the time-dependent  $CP$  violation measurement is also a good approach to check the effect from NP by comparing its result with the one of tree-dominant  $B^0 \rightarrow J/\psi K^0$  mode. We are also interested in the longitudinal polarization fraction ( $f_L$ ) in the vector-vector  $B \rightarrow \phi K^*$  decays. Previous measurements on  $f_L$  of  $B^0 \rightarrow J/\psi K^0$  show sizable contribution from transverse polarization, while the longitudinal polarization is predicted to be dominant. Although this effect can be theoretical understood nowadays [3, 4], the  $f_L$  measurement is still important to check the effects from non-uniform detector acceptance.

SuperKEKB [5] is an asymmetric  $e^+e^+$  collider, and it started the collision operations with the Belle II detector [6] from March 2019. We utilize a skimmed good-quality data sample of  $34.6 \text{ fb}^{-1}$ , which was collected at the  $\Upsilon(4S)$  resonance up to June 2020. This report will present the first reconstruction of 12 charmless  $B$  decays with Belle II data:  $B^0 \rightarrow K^+\pi^-$ ,  $B^0 \rightarrow \pi^+\pi^-$ ,  $B^+ \rightarrow K^+\pi^0$ ,  $B^+ \rightarrow \pi^+\pi^0$ ,  $B^+ \rightarrow K^0\pi^+$ ,  $B^0 \rightarrow K^0\pi^0$ ,  $B^+ \rightarrow K^+K^-K^+$ ,  $B^+ \rightarrow K^+\pi^-\pi^+$ ,  $B^0 \rightarrow \phi K^0$ ,  $B^+ \rightarrow \phi K^+$ ,  $B^0 \rightarrow \phi K^{*0}$ , and  $B^{*+} \rightarrow \phi K^{*+}$  [7, 8]. The measurement results on their branching fractions,  $CP$  asymmetries (of some of the decays above with flavor-specific final state), and  $f_L$  of two  $B \rightarrow \phi K^*$  decays will be reported.

## 2. $B$ candidate reconstruction and event selection

The  $B$  reconstruction, event selection criteria, and background suppression scheme are studied with various MC simulation samples for both signal decays and background. Charged tracks are identified with inner vertex detectors and Central Drift Chamber with requirements on the impact parameters to reduce beam-background-induced tracks. The identification of charged particle utilizes the information from two PID devices in different regions of Belle II: Time-Of-Propagation Counter in barrel region and Proximity focusing Aerogel Ring Image Cherenkov Counter in forward endcap region.  $\pi^0$  candidate is reconstructed by using two isolated clusters in the Electromagnetic Calorimeter, with requirements on the helicity angle and kinematic fit to constrain  $\pi^0$  mass.  $K_S^0$  candidate is reconstructed with two opposite-charged pion tracks from a common vertex, and there are additional requirements on its kinematic variables, e.g. momentum, flight distance, distance between 2 pions' trajectories, etc, to further reduce the combinatorial background.  $\phi$  candidate is reconstructed with two opposite-charged Kaon tracks.  $K^{*0}$  is reconstructed with one  $K^+$

and one  $\pi^-$ , and  $K^{*+}$  is reconstructed with one  $K_S^0$  and one  $\pi^+$ . In the three-body decays, there are obvious peaking backgrounds from charmed or charmonium intermediate states at two-body invariant masses, e.g.  $D^0 \rightarrow K^- \pi^+$ ,  $\eta_c \rightarrow \pi^+ \pi^-$ , etc. The corresponding mass windows of those peaks are vetoed.

We use the following two major variables to distinguish the signal  $B$  events from other backgrounds:

- $\Delta E \equiv E_B - \sqrt{s}/2$ : Energy difference between the reconstructed  $B$  candidate and half of the collision energy in  $\Upsilon(4S)$  frame.
- $M_{bc} \equiv \sqrt{s/(4c^2) - (p_B^*/c)^2}$ : Beam-energy-constrained mass.

### 3. Continuum background suppression

Due to small branching fraction ( $O(10^{-5})$ ), one of the main challenges of the charmless  $B$  decays' search is the large combinatorial background with the same final state from the  $e^+e^- \rightarrow q\bar{q}$  ( $q = u, d, s, c$ ) processes. In addition to the  $K/\pi$  suppression with PID devices, the other key is using multivariate method based on the event topological difference between the jet-like  $q\bar{q}$  events and spherical shape  $B$  decays. A binary boosted decision-tree (BDT) classifier is utilized to combine more than 30 variables nonlinearly. The input variables to BDT include event topology variables, flavor-tagging information, vertex-fitting information, and kinematic-fit information. All of them are required to be loosely or not corrected to  $\Delta E$  and  $M_{bc}$ . Figure 1 shows the performance of the BDT discriminator. The selection on the BDT output classifier ( $C_{out}$ ) is optimized by using MC samples, and is validated by using  $B^+ \rightarrow \bar{D}^0 \pi^+$  control sample.

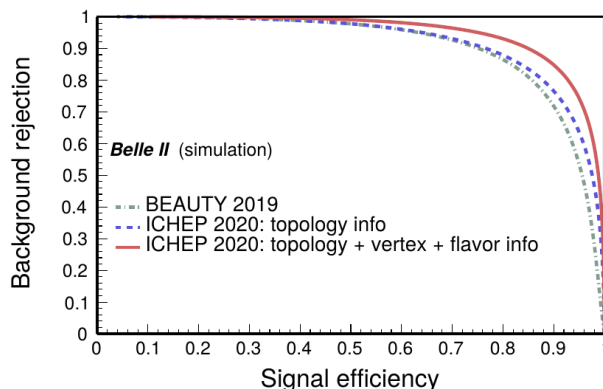


**Figure 1:** Performance of the BDT discriminator with selecting different sets of input variables.

### 4. Signal extraction and measurement results

We use unbinned maximum likelihood fit to extract numbers of signal yield from the data sample to calculate various physics observables. In addition to  $\Delta E$  and  $M_{bc}$ , there are five more variables involved in the fit:

- $C'_{out}$ : Transformed output of the continuum suppression BDT discriminator  $C_{out}$ .
- $m_{K^+K^-}$ :  $\phi$  candidate's invariant mass.
- $\cos\theta_{H,\phi}$ :  $\phi$  candidate's cosine of the helicity angle.
- $m_{K\pi}$ :  $K^*$  candidate's invariant mass.
- $\cos\theta_{H,K^*}$ :  $K^*$  candidate's cosine of the helicity angle.

The two  $B \rightarrow \phi K^*$  modes use all the seven variables above; the two  $B \rightarrow \phi K$  modes use five variables excluding  $m_{K\pi}$  and  $\cos\theta_{H,K^*}$ ; and the rest of the modes use  $\Delta E$  only with  $M_{bc} > 5.27 \text{ GeV}/c^2$  in the data fit.

After obtaining the signal yields by fitting on data, we calculate the following physics observables:

- Branching fraction:  $\mathcal{B} = \frac{N}{\varepsilon \times 2 \times N_{BB}}$ , where  $N$  is the signal yield,  $\varepsilon$  is the signal reconstruction efficiency, and  $N_{BB}$  is the number of  $B\bar{B}$  events.
- $CP$  asymmetry: The raw asymmetry is obtained by  $\mathcal{A} = \frac{N(b) - N(\bar{b})}{N(b) + N(\bar{b})}$ , where  $N(b)$  and  $N(\bar{b})$  are the yields of the final state with  $b$  and  $\bar{b}$  flavors, respectively. The  $CP$  asymmetry can be obtained by considering the instrumental effect:  $\mathcal{A} = \mathcal{A}_{CP} + \mathcal{A}_{det}$ .
- Logitudinal polarization fraction:  $f_L = \frac{N_L/\varepsilon_L}{N_L/\varepsilon_L + N_T/\varepsilon_T}$ , where  $N_{L(T)}$  and  $\varepsilon_{L(T)}$  is the signal yield and signal reconstruction efficiency with longitudinal (transverse) polarization, respectively. Since the two polarizations show different distribution in the two helicity angles, the probability density function (PDF) corresponding to signal can be separated into two components as shown in Figure 2.

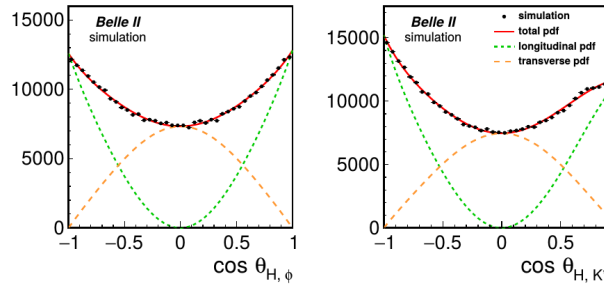


**Figure 2:** Distributions of  $\cos\theta_{H,\phi}$  and  $\cos\theta_{H,K^*}$  from MC sample. The green dashed (orange long dashed) lines are the PDFs of the longitudinal (transverse) components.

Figure 3~6 show the data fit results of  $B^0 \rightarrow K^+ \pi^-$ ,  $B^0 \rightarrow \pi^+ \pi^-$ ,  $B^+ \rightarrow K^+ \pi^0$ ,  $B^+ \rightarrow \pi^+ \pi^0$ ,  $B^+ \rightarrow K^0 \pi^+$ ,  $B^0 \rightarrow K^0 \pi^0$ ,  $B^+ \rightarrow K^+ K^- K^+$  and  $B^+ \rightarrow K^+ \pi^- \pi^+$ , projecting to  $\Delta E$ . Figure 7 shows the five dimensional fit results of  $B^+ \rightarrow \phi K^+$  and  $B^0 \rightarrow \phi K^0$ . Figure 8 shows the seven dimensional fit results of  $B^+ \rightarrow \phi K^{*+}$  and  $B^0 \rightarrow \phi K^{*0}$ . All the measurement results are summarized in Table 1.

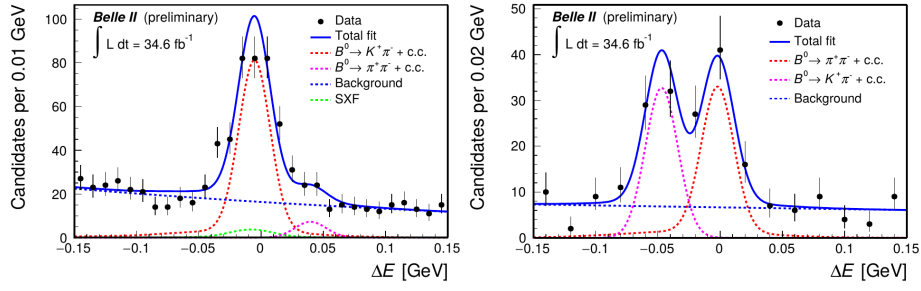


**Figure 3:** Data fit results of  $B^0 \rightarrow K^+ \pi^-$  (left) and  $B^0 \rightarrow \pi^+ \pi^-$  (right) reconstructed candidates with projecting to  $\Delta E$ .

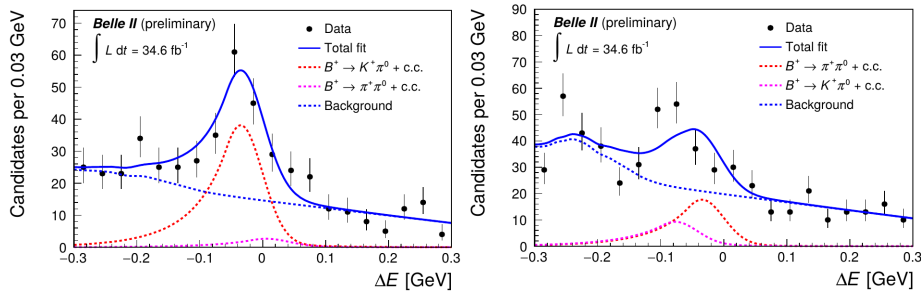


**Figure 4:** Data fit results of  $B^+ \rightarrow K^+ \pi^0$  (left) and  $B^+ \rightarrow \pi^+ \pi^0$  (right) reconstructed candidates with projecting to  $\Delta E$ .

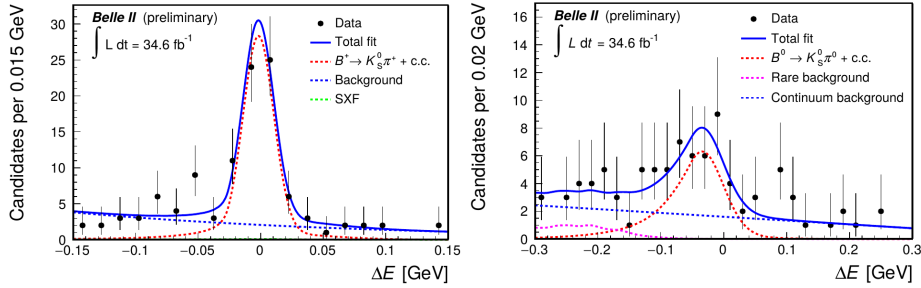


**Figure 5:** Data fit results of  $B^+ \rightarrow K^0 \pi^+$  (left) and  $B^0 \rightarrow K^0 \pi^0$  (right) reconstructed candidates with projecting to  $\Delta E$ .

## 5. Summary

Belle II performs the first reconstruction of charmless  $B$  decays with a data sample of  $34.6 \text{ fb}^{-1}$ . The measurements include branching fraction,  $CP$  asymmetry, and longitudinal polarization fraction of  $B \rightarrow \phi K^*$  modes. All the rediscovery results are in agreement with the present world average values, and are good validations on the detector system performance and analysis strategies. As the integrated luminosity will soon reach order of  $\text{ab}^{-1}$  in coming years, Belle II is ready for new physics hunting.

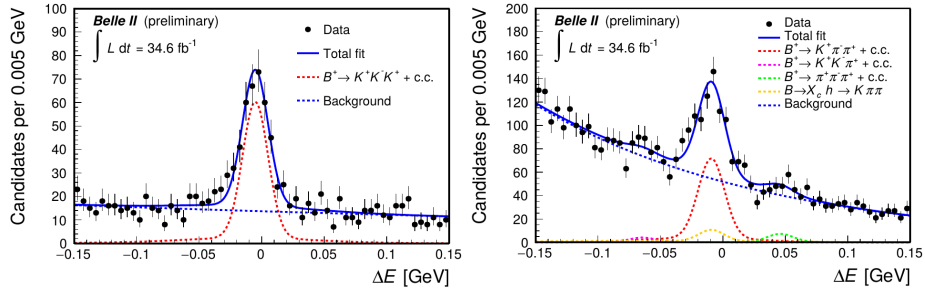


**Figure 6:** Data fit results of  $B^+ \rightarrow K^+K^-K^+$  (left) and  $B^+ \rightarrow K^+\pi^-\pi^+$  (right) reconstructed candidates with projecting to  $\Delta E$ .

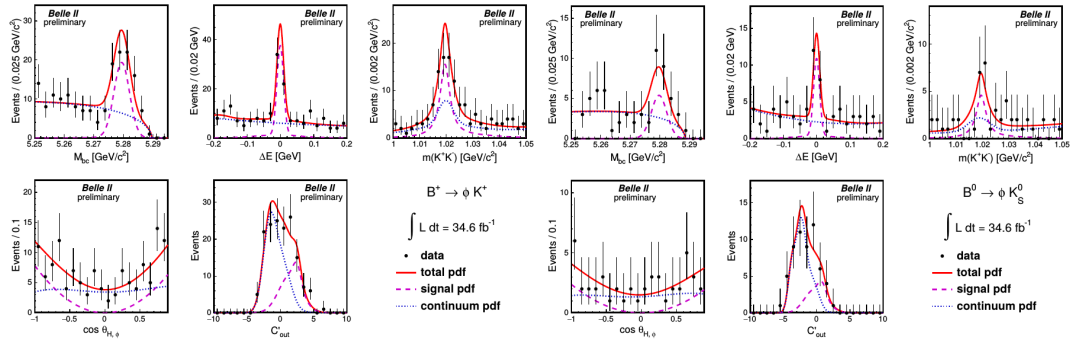


**Figure 7:** Data fit results of  $B^+ \rightarrow \phi K^+$  (left) and  $B^0 \rightarrow \phi K^0$  (right) reconstructed candidates with projecting on  $\Delta E$ ,  $M_{bc}$ ,  $C'_{out}$ ,  $m_{K^+K^-}$ , and  $\cos\theta_{H,\phi}$ .

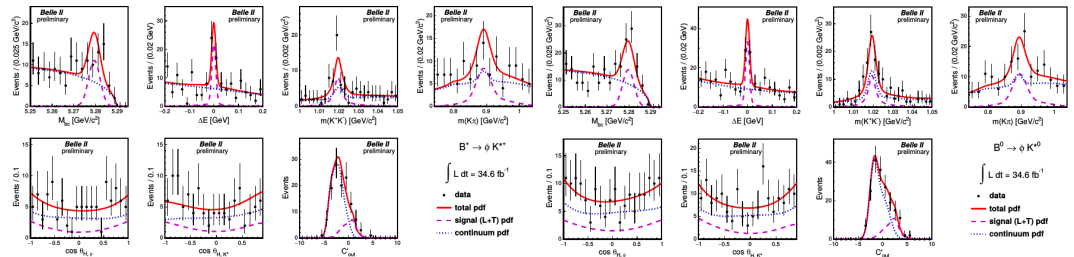


**Figure 8:** Data fit results of  $B^+ \rightarrow \phi K^{*+}$  (left) and  $B^0 \rightarrow \phi K^{*0}$  (right) reconstructed candidates with projecting on  $\Delta E$ ,  $M_{bc}$ ,  $C'_{out}$ ,  $m_{K^+K^-}$ ,  $\cos\theta_{H,\phi}$ ,  $m_{K\pi}$ , and  $\cos\theta_{H,K^*}$ .

## References

- [1] M. Gronau and D. London, Phys. Rev. Lett. **65**, 3381 (1990).
- [2] M. Gronau, Phys. Lett. B **627**, no. 1, 82-88 (2005).
- [3] A. L. Kagan, Phys. Lett. B **601**, 151 (2004).
- [4] M. Beneke, J. Rohrer, and D. Yang, Phys. Rev. Lett. **96**, 141801 (2006).
- [5] K. Akai *et al.*, Nucl. Instrum. Meth. A **907** 188-199 (2018).

**Table 1:** Summary of measurement results. The first errors in the values are statistical and the second ones are systematic.

Mode	$\mathcal{B}$ ( $10^{-6}$ )	$\mathcal{A}_{CP}$	$f_L$
$B^0 \rightarrow K^+ \pi^-$	$18.9 \pm 1.4 \pm 1.0$	$0.030 \pm 0.064 \pm 0.008$	-
$B^0 \rightarrow \pi^+ \pi^-$	$5.6^{+1.0}_{-0.9} \pm 0.3$	-	-
$B^+ \rightarrow K^+ \pi^0$	$12.7^{+2.2}_{-2.1} \pm 1.1$	$0.052^{+0.121}_{-0.119} \pm 0.022$	-
$B^+ \rightarrow \pi^+ \pi^0$	$5.7 \pm 2.3 \pm 0.5$	$-0.268^{+0.249}_{-0.322} \pm 0.123$	-
$B^+ \rightarrow K^0 \pi^+$	$21.8^{+3.3}_{-3.0} \pm 2.9$	$-0.072^{+0.109}_{-0.114} \pm 0.024$	-
$B^0 \rightarrow K^0 \pi^0$	$10.9^{+2.9}_{-2.6} \pm 1.6$	-	-
$B^+ \rightarrow K^+ K^- K^+$	$32.0 \pm 2.2 \pm 1.4$	$-0.049 \pm 0.063 \pm 0.022$	-
$B^+ \rightarrow K^+ \pi^- \pi^+$	$48.0 \pm 3.8 \pm 3.3$	$-0.063 \pm 0.081 \pm 0.023$	-
$B^0 \rightarrow \phi K^0$	$5.8 \pm 1.8 \pm 0.7$	-	-
$B^+ \rightarrow \phi K^+$	$6.7 \pm 1.1 \pm 0.5$	-	-
$B^0 \rightarrow \phi K^{*0}$	$11.0 \pm 2.1 \pm 1.1$	-	$0.57 \pm 0.20 \pm 0.04$
$B^{*+} \rightarrow \phi K^{*+}$	$21.7 \pm 4.6 \pm 1.9$	-	$0.58 \pm 0.23 \pm 0.02$

[6] T. Abe *et al.* (Belle II Collaboration), arXiv:1011.0352.

[7] F. Abudinén (Belle II Collaboration), arXiv:2009.09452.

[8] F. Abudinén (Belle II Collaboration), arXiv:2089.03873.